IMPORTANT PARAMETERS OF LASER WELDING FOR METALLIC MATERIALS INTERCONNECT IN FUEL CELL: A SHORT REVIEW

Mohd Faizal Tukimon[1], Hamimah Abd. Rahman[1*], Shahrin Hisham Amirnordin[1], Umira Asyikin Yusop[1], Zolhafizi Jaidi[1], Azzura Ismail[1], Sufizar Ahmad[1] and Aiman Mohd. Halil[2]

[1]Faculty of Mechanical and Manufacturing Engineering, Universiti Tun Hussein Onn Malaysia, 86400 Parit Raja, Batu Pahat, Johor, Malaysia.
[2]Faculty of Mechanical & Automotive Engineering Technology, Universiti Malaysia Pahang, 26600 Pekan, Pahang, Malaysia

*hamimah@uthm.edu.my

Abstract. The development of laser welding application is a critical innovation in accomplishing urbanity objectives whilst guaranteeing first-class measures for mechanical and electrical associations to generate electro-mobility components. Generally, laser welding application is utilized for cutting metals, fabricating cell containers, and fuse conductor materials to battery and fuel cell applications. However, the application of laser welding has some constraints in parameter settings, such as laser beam oscillation, welding power, and speed, thereby indicating a different mechanical and morphology analysis. Several results of welding analysis have been reviewed from the previous research to identify the best parameter for laser welding application with metallic materials. Amongst the parameters studied, infinity laser beam oscillation is the best parameter for minimizing porosity in the welding area, hence increasing the mechanical properties. These mechanical properties were also proven to improve as the parameter of laser power increased. Therefore, this study can serve as a guideline in selecting suitable parameters for the application of laser welding in fuel cell interconnect metallic materials.

Keywords: Joining process, Laser welding, Metallic, Macrostructure, Microstructure

Article Info

Received 16th December 2021
Accepted 4th April 2022
Published 20th April 2022

ISSN: 1823-7010, eISSN: 2600-7444

Introduction

Recently, the growth of fuel cell technologies such as Solid Oxide Fuel Cell (SOFC) has given a favorable way to improve the performance of the system. One of the methods to improve the SOFC system is the material selection for interconnectors. The interconnector is one of the most imperative parts of the fuel cell, where it combined single cells to create a pile of fuel cells [1-2]. For the last three years, ceramic material has been used in most fuel cell applications [3-5]. However, the ceramic material is unable to operate at higher working temperatures due to its characteristic that is fragile at high temperatures [1]. Alternatively, fabricating the stainless-steel material as the new interconnect in the fuel cell system is desirable due to its characteristics such as good electrical conductivity, outstanding strength, ease of fabrication, low cost, and good mechanical properties [6]. The conventional method of welding in stainless steel, such as Tungsten Inert Gas (TIG), is the most commonly used method for fabricating stainless steel. TIG welding with low welding efficiency and high heat input, on the other hand, can easily result in large deformation and residual stress, which is disadvantageous to crack suppression [7]. Therefore, in order to fabricate the stainless-steel interconnect, a method of laser welding process needs to be conducted for joining the stainless-steel interconnect with the fuel cell application instead of the conventional method [8-9].

The application of laser welding has been broadly utilized in the different manufacturing industries, because of its advantages in realizing extra production, automotive works, and forming a good-quality of weld with small heat-affected zones (HAZs) [10-11]. The principle of laser welding authorized the preparation of material in the micron range but, at the same time, it had diminished the quality on the surface of prepared parts [12-13]. Furthermore, laser welding has a higher power density resulting in the interaction between the welded material being indestructible, mainly within the profound perforation welding on a solid plate. In recent years, the demand for this application has increased due to the diminished fossil fuel consumption in the electrical power supply application [14-15]. Therefore, some reviews of laser welding on different parameters for different types of metallic material are essential to develop high-quality products in various applications.

According to previous studies, laser welding with the characteristic of high energy density and the little heat-influenced zone has ended up as an attractive operation to the conventional method of joining metallic materials [16-17]. Nevertheless, during the operation of laser welding, the performance of the welded material has been depleted due to some issues such as incomplete penetration, porosity, and cracking. Several studies on the manufacturing of different types of metallic material have been a crisis in performing the laser welding operation due to the selection of suitable parameters [18-24]. Usually, the welding defects occurred due to the unsuitable condition used in the laser welding operation. This situation may lead to the production of incompetent products resulting in huge losses to the industry. Therefore, in order to maintain the consistency of fabrication in the industry, the preliminary operation needs to be done by selecting good welding conditions for laser welding.

The laser welding application has two crucial parts which are the laser beam and metallic materials. The procedure of laser welding starts as the laser beam shot down to the surface of metallic material through the optical fiber and lens. Reasonable parameters for laser welding innovation should be determined to form a good welded joint for industrial applications, such as battery and fuel cells. This study focuses on understanding the

parameter of laser welding and the consequence to the welded area. Therefore, proposing the best parameters of laser welding will enhance future development in metallic material for interconnect in SOFC.

Laser Welding

Principle of laser welding. According to previous studies, the basic mechanism of the application of laser welding is that the specimen was welded through the penetration of a laser beam that vaporizes the welded area and produces a keyhole in the middle of the molten puddle. The schematic of the formation of keyholes through laser beam penetration is represented in Figure 1.

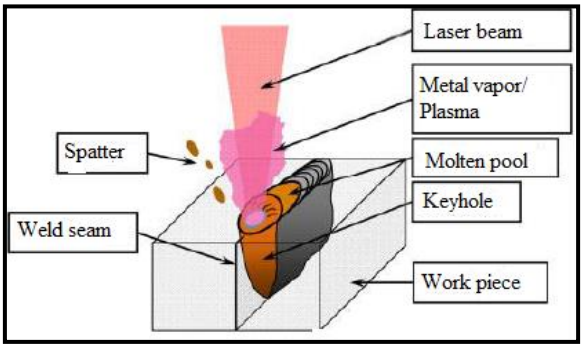

Figure 1. Formation of keyhole [10]

During the formation of keyholes in the material, a light smoke containing metallic vapor and plasma was produced and dissipated to the surrounding, as shown in Figure 1. A comparison between the traditional welding innovation and the proposed approach indicated that the penetration through laser welding operation is caused by the laser beams that travel along with the optical fiber and lens [11], thereby resulting in the formation of keyholes. According to previous studies, there are two mechanisms that have been found in the operation of laser welding which are heat conduction and deep penetration welding [25]. Figure 2 shows the system of heat conduction and deep penetration in laser welding.

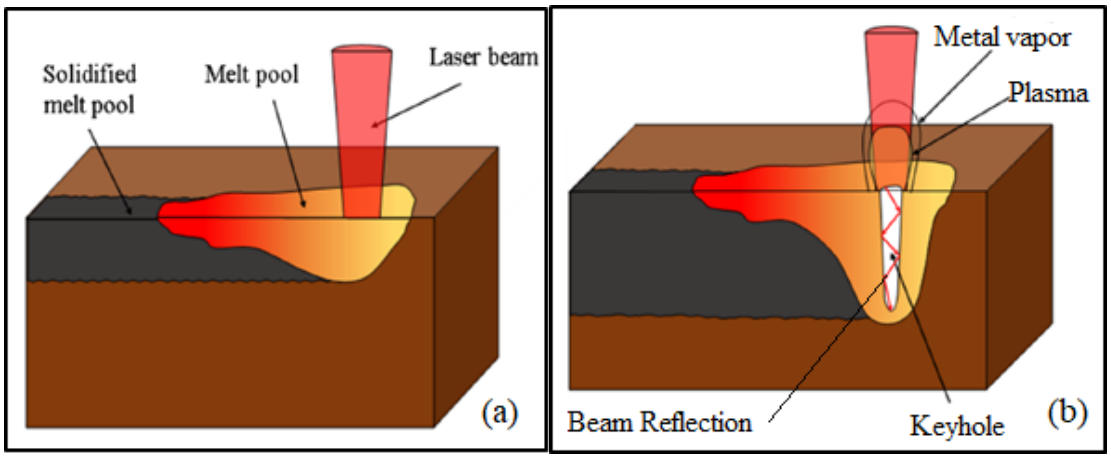

Figure 2. (a) Mechanism of heat conduction and (b) Mechanism of deep penetration [25]

As shown in Figure 2(a), the area of welded area is dissolved and the energy is moved into more profound layers through heat conduction. The deep penetration welding system indicates the formation of keyholes due to the increment intensity of the radiation that causes the material to change to a vaporous condition. Continuous laser beam penetration is reflected inside the keyhole, increasing the intensity of the operating parameter, as shown in Figure 2(b). As the intensity increases, the probability that the materials will melt is high, resulting in deeper penetration. Therefore, a stronghold between the welded part and the material has been generated.

Parameter of Laser Welding

Type of oscillation. Laser oscillating welding, a promising welding method with high efficiency and adaptability, can produce laser beam stirring molten pools with different oscillating modes. The oscillation effect can alter the rate of solidification of a molten pool, hence improving the microstructure and decreasing deformation in the welded area. Previous researchers claim that by using circular laser oscillation to weld stainless steel SUS304, they discovered that moving the circular oscillation could cause a cyclical drag force on the keyhole-melt interface and lower the peak temperature and temperature gradient [26]. Other studies have used the transverse laser oscillating to weld SUS304 stainless steel. They discovered that the aspect ratio of columnar crystal grain size was reduced by 36%, while the micro-hardness and strength of the welded joint were slightly increased [27]. Furthermore, different types of laser beam oscillating have helped to reduce defects during laser welding processes, according to previous studies. Figure 3 shows the defect that might exist during laser welding analysis.

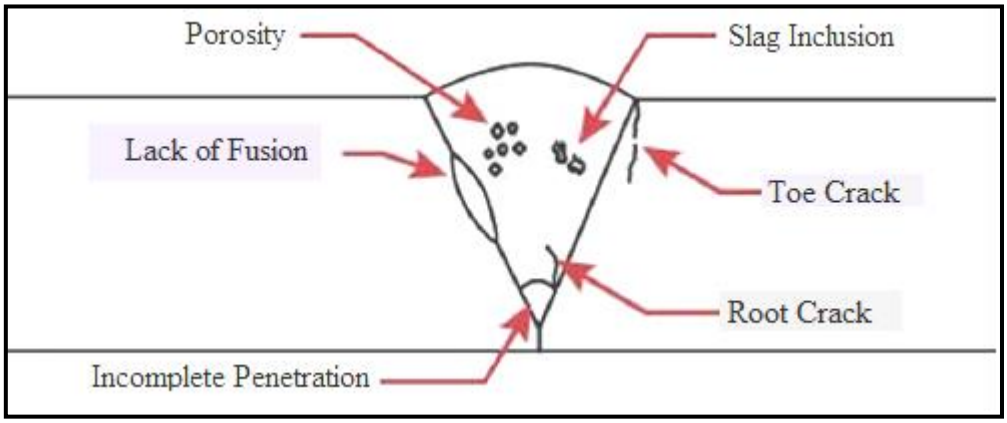

Figure 3. Example of laser welding defect [28]

The defects shown in Figure 3 indicate that any potential weld defect can affect the mechanical properties of the material. For example, the unbalanced morphology contamination on the welded area and alteration of laser beam properties results in unacceptable products for manufacturing purposes [28]. Furthermore, the welded area with defects increases the risk of failure in the application. Therefore, the best parameter of laser welding should be investigated to minimize the defects in the welded area.

As shown in Figure 4, the studies on different oscillation on high-strength stainless steel have been used which are without, transverse, longitudinal, circular oscillation. The

width and length of the oscillating beam were set to 2 mm, while the laser power and welding speed were set to 3.2 kW and 4 mm/s, respectively. Furthermore, Argon (Ar) gas is used as a protective gas for both upper and root protection of the samples, with flow rates of 20 L/min. Figure 5 shows the macrostructure analysis on the surface and the cross-sectional of the welded area produced by different types of laser oscillation.

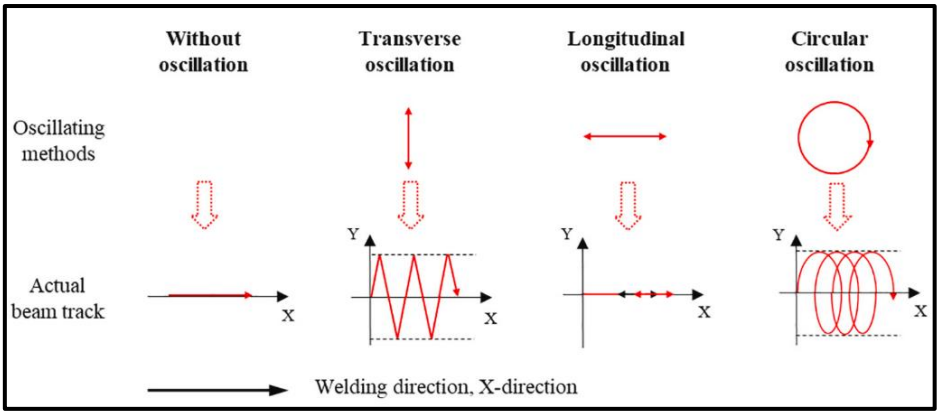

Figure 4. Type of oscillation mode and actual beam direction [7]

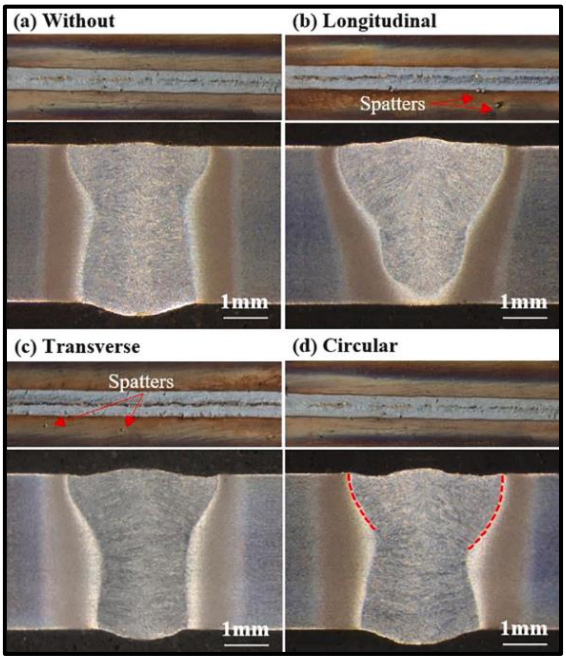

Figure 5. Macrostructure of the surface and weld cross-sections produced by different laser oscillating [7]

Based on the comparison of macrostructure analysis in Figure 5, it is shown that the surface of welded area for transverse and longitudinal oscillation has resulted some spatters. Meanwhile, the welded area was relatively smooth and clean, both without oscillation and circular oscillation. Furthermore, the difference in cross-section morphology of the four welding modes was more significant. The longitudinal oscillation weld was showing an incomplete penetration, whereas the welds in the other oscillating modes were all fully penetrated. However, as seen in the cross-sectional diagram for circular oscillation, the shape

of the depth of penetration is not symmetric due to the different energy distribution of the laser beam on both sides of the weld during the welding process [29]. As a result, it is also critical to ensure that the angle of the laser beam is stable on both sides to avoid such defects.

In other studies from the previous study, there are several types of laser beam protocol which are linear laser beam oscillation, circle laser beam oscillation, and infinity laser beam oscillation. According to Wang et al., the base material used is 5A06 Aluminium, and an IPG-6000 fiber laser with a D50 wobble seam oscillation head is used [30]. The parameter of the process is configured as shown in Table 1.

Table 1. Parameter of laser welding [30]

	Parameter
Type of oscillation	Linear, Circle, Infinity
Laser power	4000 W
Spot diameter	0.4 mm
Welding speed	1800 mm/min
Gas	99.99 % of Argon gas
Flow rate	15–18 L/min

A preliminary step to immerse the bead on the aluminium plate with acid is necessary to remove any impurities on the surface before the welding process. Then, the welding was performed in a straight line [30-31] on the top of the aluminium base material. Figure 6 shows the different appearances of welded lines in each condition.

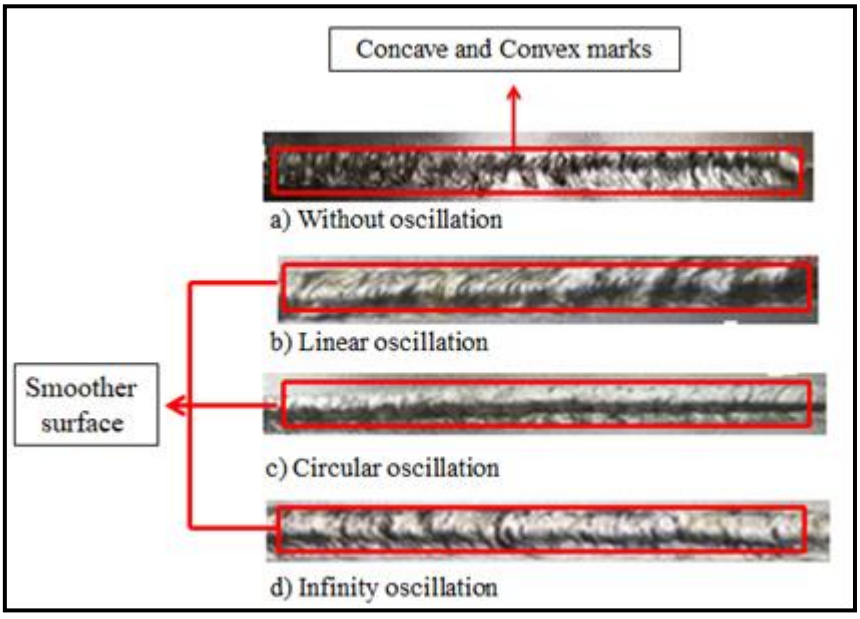

Figure 6. Observation of laser welding with different types of oscillation [30]

Figure 6 shows that the laser beam with oscillation has a better appearance than the laser beam without oscillation. For the laser beam without oscillation process, the surface of the welded area has a clear concave and convex mark, and the laser beam with oscillation has a smooth surface welded area. However, the cross-sections of the weld for linear, circle, and infinity oscillating techniques have welding pores. The weld has toe and root defects were

caused by the Marangoni effect within the weld pool [30-32]. It is also shown that the size of pores decreased from infinity oscillation < circle oscillation < linear oscillation < without oscillation. Consequently, the parameter type of laser beam oscillation has been assumed to control the formation of pores in the fusion area.

According to previous studies, the presence of pores inside the welded area is due to some cases shown in Figure 7.

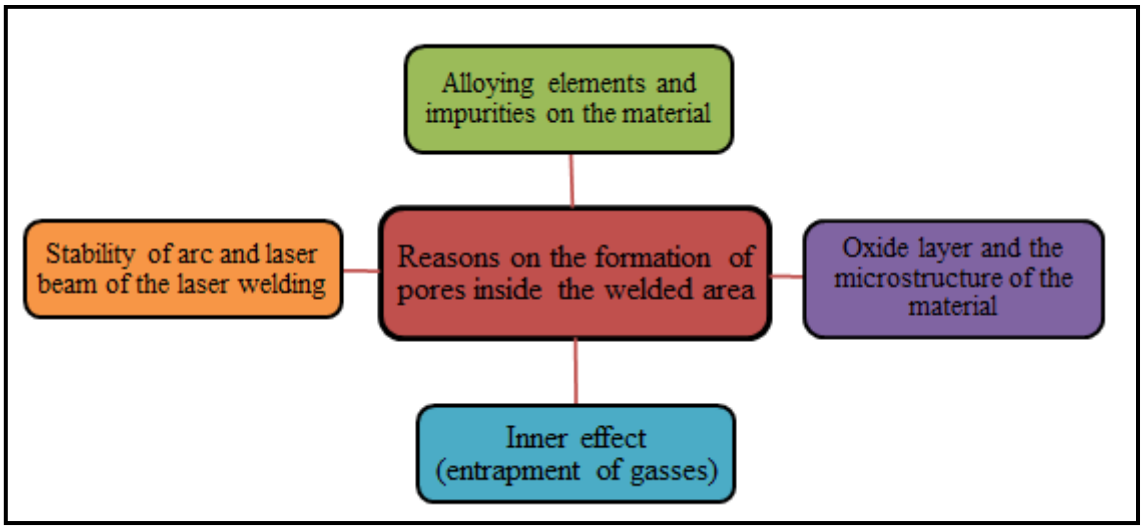

Figure 7. Main causes for the existence of pores inside the welded area are illustrated in the mind map [36]

According to previous studies, the common reasons for the formation of pores inside the welded area are illustrated in Figure 7. The existence of impurities has affected the stability of the keyhole on the surface of the material. Unwanted materials are observed inside the welded area during the microstructure analysis. The position and the angle of the laser beam should be perpendicular to the welded zone to avoid the beam being distorted from the targeted welded area [30]. The protecting gas inside the welded area also contributed to securing the melted pool, but it is also captured within it resulting rapid coagulation. In addition, the characterization of metallic material, particularly the martensitic composition, can trigger the distribution of the pores by bringing them to the tips of the dendritic composition [36]. Therefore, avoiding these possibilities on the formation of pores on the welded material can reduce the pore from appearing during the laser welding process.

The microstructure analysis has been conducted using scanning electron microscopy (SEM) to provide a sharp vision of the morphology of the welded area. The microstructure analysis of the presence of dendrite is shown in Figure 8. Figure 8(b) to Figure 8(e) show the presence of $\beta(Mg_3Al_2)$ dendrites in the welded region. Meanwhile, Figure. 8(a) and (f) show that no $\beta(Mg_3Al_2)$ is formed because of increasing heat input and rate of super-cooling through the laser welding operation [30]. Another researcher has supported the statement that the non-existence of this dendrite was mainly due to the degree of supercooling during the laser welding process [31].

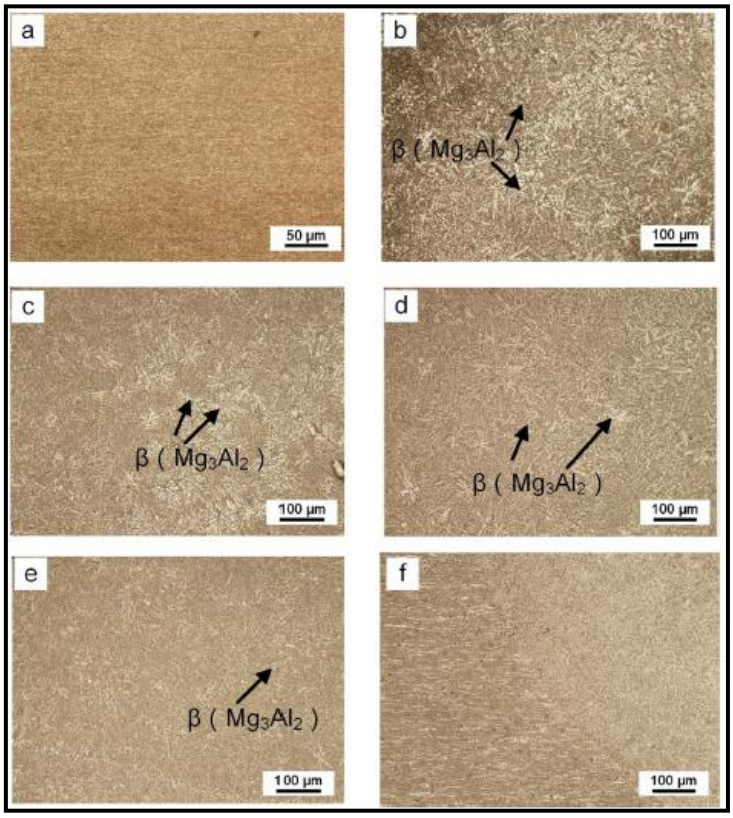

Figure 8. Morphology on the base material (a) raw material (b) fusion zone (FZ) without laser beam oscillation (c) FZ with linear laser beam oscillation (d) FZ with circle laser beam oscillation (e) FZ with infinity laser beam oscillation and (f) heat affected zone (HAZ) with infinity oscillation [30]

A non-oscillation laser beam shows an inconsistent distribution of dendrite compared with other oscillation types. On the other hand, the reflection inside the keyhole throughout the laser welding procedure is the main reason for the uniform distribution of β(Mg_3Al_2). It is also supported that the effect of laser oscillation has refined the grains and promoted the uniform distribution of the β(Mg_3Al_2) phase in the weld fusion zone [31]. The effect on the existence of β element has led to the increase of microhardness and the strength of the metallic alloy respectively. It is also mentioned that the percentage of a porous element in the weld with oscillation is less than the material without oscillation. Hence, the microstructure of the materials has improved from infinity oscillation > circle oscillation > linear oscillation > without oscillation because the distribution of β(Mg_3Al_2) dendrite is more uniform. As a result, the parameter of the laser welding oscillation beam has been assumed to control the formation of defects in the fusion area.

Laser power. Despite the increasing demand for using laser welding in manufacturing industries, the knowledge about the joining parameter is limited. A review of the parameter of laser power should be investigated to improve the mechanical properties of materials. According to a previous study, the use of laser power 400 W and 600 W is illustrated by Figure 9. This study has used material of stainless-steel grading AISI 304 with and without metal powder that acts as filler.

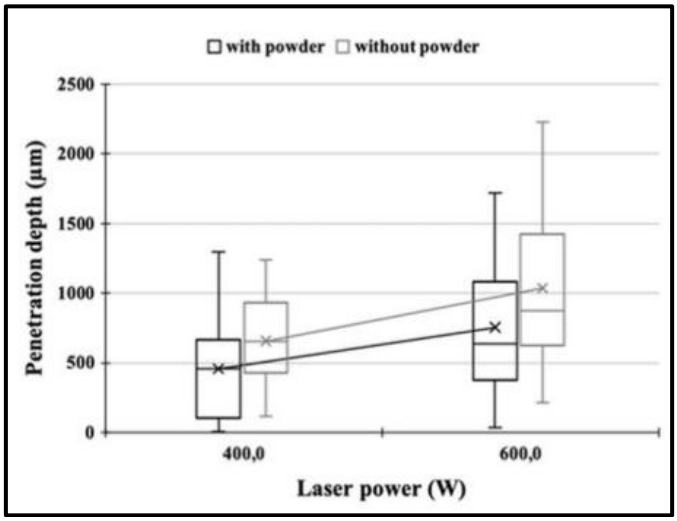

Figure 9. Depth of penetration for different laser power [32]

Figure 9 depicts the depth of penetration for various laser powers used with and without powder. Because of the increased heat source, the depth of penetration has increased. However, only the microstructure analysis of laser power of 600 W has been discussed and illustrated in Figure 10. There is a fusion line at the interface between the base material and the molten zone, and a typical cellular growth has been discovered. Because the heat-affected zone (HAZ) was so thin, it could not be resolved. Figure 10 depicts a columnar dendritic microstructure directed towards the solidification direction at the interface as a result of the stainless steel's rapid solidification. This has proved that the increase in laser power has led to the fine distribution of grain at the welded area, hence improving the properties at the welded area [33-35].

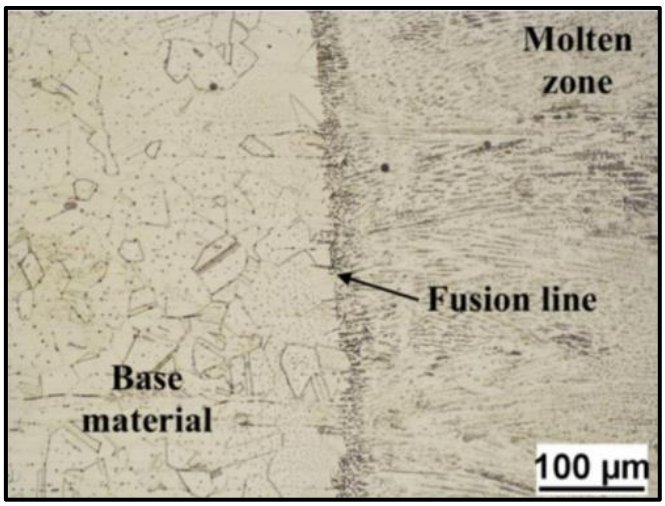

Figure 10. Cross-section of the fusion boundary for laser power 600W [32]

Several studies investigated the laser power of laser welding also has been done on metallic alloy materials. Previous studies have mentioned the combination of five millimeters (5mm) thick Ti-6A1-4V using laser welding with the variable of different range of laser

power (P) with constant welding speed and defocused distance. The list of variables is tabulated in Table 2.

Table 2. Variable for the laser welding process [38]

Number	Power, P (W)	Speed, S (mm/min)	Defocussed distance, F (mm)
1	1500	300	2
2	1600		
3	1700		
4	1800		
5	1900		

Preliminary testing using laser power of 1200 W to 1500 W has found that the depth penetration increased up to 80% as the laser power increased to 1500 W. The parameter of laser power to create a minimum penetration of approximately 80% in the bead on plate of Ti-6A1-4V alloy is listed according to Table 2. The results are according to the fusion zone (FZ), heat affected zone (HZ), and penetration depth (d) are illustrated in Figure 11.

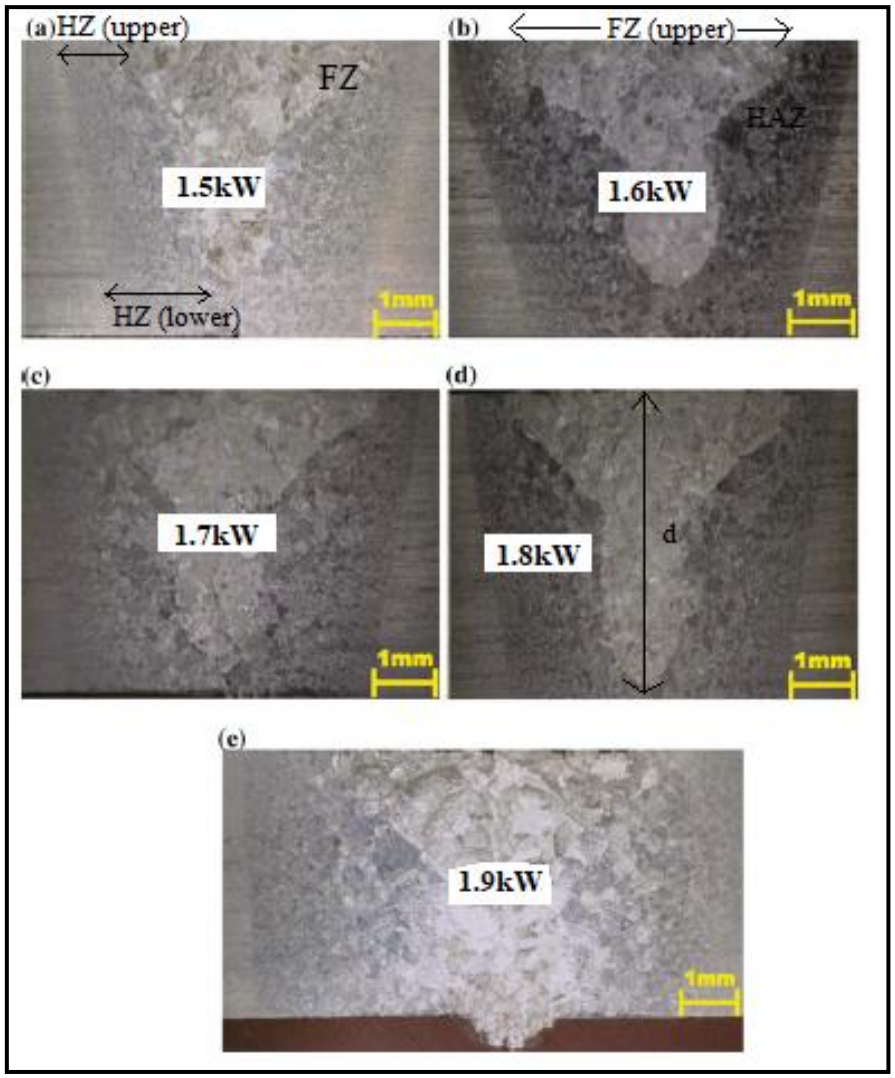

Figure 11. Appearance of weld at various laser power (a) 1.5kW, (b) 1.6kW, (c) 1.7kW, (d) 1.8kW and (e) 1.9kW [38]

In particular, lowering the laser power has reduced the heat resulting in incomplete penetration at the welded area. The depth of penetration has become a significant factor influencing the appearance of defects that can be observed in the cross-sectional welded area. Based on Figure 11, as the laser power increased from 1.5 kW to 1.9 kW, the depth of penetration has also increased. According to previous studies, the power density has arisen as the laser power is elevated [39-41]. Therefore, the laser beam of laser welding has executed a high-power density on the welded material. It is known that the low laser power is insufficient to create a keyhole at the bottom of the welded area [44], hence making the welded part not distributed evenly. However, it is also shown that as the laser power is elevated, the FZ on the upper surface has also increased due to the presence of a plasma cloud on top of the material surface. The plasma cloud that consists of metallic vapor has absorbed the power of the laser beam and reflects the heat on top of the surface, thereby increasing the width of FZ. The pressure was reflected inside the keyhole and created a molten pool from the bottom to the upward surface due to the Marangoni effect [30, 37-38]. Therefore, the width of FZ on the upper surface increased. On the contrary, the HAZ on the lower base material also provided important knowledge because its microstructure was changed after the laser welding operation. The size of HAZ were depending on the characteristic of the thermal conductivity of the material. Ti64 has a low thermal conductivity of approximately 6.7 W/mK; thus, the cooling rate of the material is lower than the material that possesses high thermal conductivity, such as stainless steel [38-40]. Therefore, a suitable material that possesses high thermal conductivity that can replace Ti64 should be evaluated to improve several industries, such as fuel cell and automotive.

Welding speed. The application of laser welding is a preferable method of joining operations in several industries like aerospace and fuel cell. In general, unsuitable parameters or welding condition leads to imperfection, such as pores, and incinerated surface on the welded area or insufficient welding penetration. Several analyses have been conducted to identify the best parameter for laser welding application. Table 3 shows the parameters that use different values of welding speed on 3 mm thickness of Ti6A14V alloy material.

Table 3. Parameter of laser welding [43]

Parameter	Sample				
	1	2	3	4	5
Laser Power	1.8kW	1.9kW	2.0kW	2.1kW	2.2kW
Pulse duration	7.0ms	8.0ms	9.0ms	10.0ms	11.0ms
Welding speed	3.0mm/s	4.0mm/s	5.0mm/s	6.0mm/s	7.0mm/s

According to Table 3, it is shown that the welding speed escalated from 3.0 to 7.0 mm/s, resulting in the temperature around the FZ decreasing to almost 230 ℃. However, this condition drastically lowered the tensile strength of the material to approximately 20%. Mechanical testing analysis was conducted through analysis of variance (ANOVA) testing [43-45]. The result regarding the parameters on the tensile test from ANOVA is represented in Figure 12.

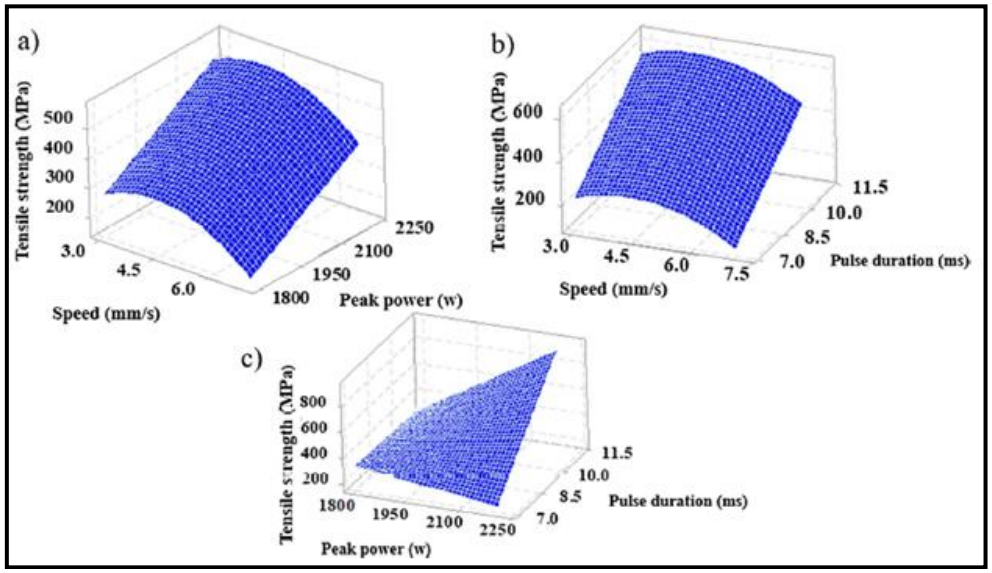

Figure 12. The result of tensile strength (a) speed and peak power, (b) speed and pulse duration and (c) peak power and pulse duration [43]

As the value of welding speed accelerated from the lowest to the highest speed, it has negatively affected the tensile strength of the Ti6A14V material based on Figure 12. The strength decreased as the welding speed increased [43-45]. This phenomenon occurred due to the decrease in the number of metallic materials and the penetration rate. In addition, the size of imperfection has increased as the welding speed increases [46]. Therefore, reducing the welding speed parameter is important to minimize the defects in a laser welding application [47-48].

Previous researchers investigated the effect of laser power (2000 W, 2300 W, and 2600 W) and welding speed (1.5 m/min, 2.0 m/min, and 2.5 m/min) on the strength of austenitic stainless steel (AISI 316) and low carbon steel (AISI 1018). The dimension of 100 mm x 100 mm x 2 mm was butt welded using a CO_2 laser welding machine with a spot diameter of 0.15 mm and focused by 15–25 mm on the upper surface of the weldment. To prevent molten metal oxidation, the entire experiment was shielded with pure argon shielding gas. Tables 4 and 5 show the list of chemical compositions of both materials and their mechanical properties respectively.

Table 4. Chemical composition for AISI 316 and AISI 1018 [49]

Material	AISI316	AISI1018
C	0.24	0.12
Si	0.28	0.10
Mn	1.44	0.6
P	0.041	0.015
S	0.017	0.012
Cr	16.95	-
Mo	2.06	-
Ni	10.09	-
Fe	Balance	Balance

Table 5 Mechanical Properties of AISI 316 and AISI 1018 [49]

Mechanical Properties	AISI 316	AISI 1018
Tensile test (MPa)	615.361	457.551
Elongation percentage (%)	42.36	30.68
Microhardness (HV)	182	142

From Table 4, it can be seen that AISI 1018 has a low level of carbon (C) element and has no composition of Chromium (Cr), Molybdenum (Mo), and Nickel (Ni). Clearly, the mechanical properties of AISI 316 are superior to AISI 1018 when the microhardness profiles across the weld zone (WZ) are examined. Table 5 demonstrates that AISI 316 has greater strength than AISI 1018. Furthermore, the microhardness of the AISI 316 and AISI 1018 base metals is 182 and 142, respectively. According to the previous, the microhardness in welded metal is due to dendrites with a higher carbide being stronger compared to other materials without carbide elements [50-52]. Laser welding speed has the greatest impact on the laser welding process, followed by laser power, which has a medium impact on the welded area [46, 49]. It has been reported that as welding speed increased, the number and size of micro-voids and micro-porosity defects has also increased. This was due to the increased welding speed causing a decrease in heat input [53-55]. Furthermore, increased welding speed has resulted in the presence of micro-defects such as porosity, pores, and hot cracks in the welded part, which has harmed its mechanical properties [56-60]. Therefore, the selection of the appropriate welding speed must be done to prevent defects from occurring at the welded part of the metallic material.

Conclusion

In conclusion, different types of material will bring different analyses toward their morphology and mechanical properties. Based on the reviews, it is mentioned that metallic material that has a greater level of carbon element has more advantages in terms of mechanical properties such as tensile strength and microhardness. In a future study, an analysis of the different types of metallic material such as ferritic stainless steel (Grade SUS430) needs to be conducted by using the proposed parameter of laser welding. Figure 13 depicts a new perforated SUS430 design developed for this purpose. The chosen parameter is as follows;

1) Laser welding is laser beam oscillation: The oscillating parameters had a significant impact on the cross-sectional bead width and weld penetration. As the oscillation diameter and frequency increased, the depth of penetration has also increased.

2) Laser power: As the laser power increases, the depth of penetration has also increased due to the increment of heat source from the laser beam. Appropriate laser power is need to be pinpointed so that there is enough power in creating a suitable keyhole at the bottom of the welded area. Good laser power also has making the distribution of grain becoming smoother, hence resulting in a lower porosity on the welded area.

3) Laser welding speed: By lowering the laser welding speed can improve the distribution of heat source from laser welding to the welded part, hence lowering the defect from occurring.

These parameters are expected to provide a more comprehensive review of the properties and morphology of the new interconnect metallic material in SOFC. According to these reviews, for joining the SUS 430 stainless-steel interconnect, the parameter involving beam oscillation, high laser power, and low welding speed is proposed. This parameter is expected to provide a better understanding of the SUS430 stainless-steel properties and morphology. As a result, this set of parameters is proposed for future fabrication to improve the performance of SOFC applications while keeping costs to a minimum.

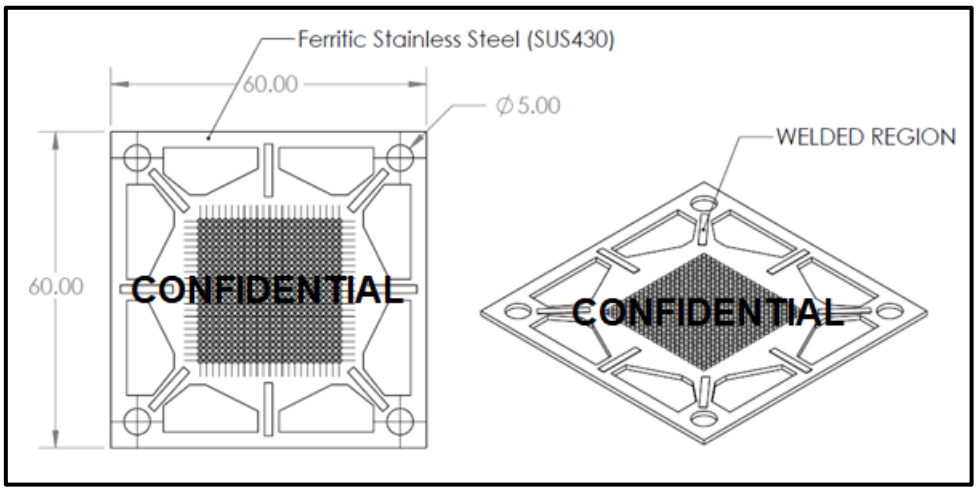

Figure 13. New design of perforated SUS430 interconnect

Acknowledgments

Researchers would like to provide appreciation to the Ministry of Higher Education Malaysia (MOHE) for the opportunity regarding towards this investigation with the Fundamental Research Grant Scheme (FRGS/1/2020/TK0/UTHM/02/15) and partly sponsored by Universiti Tun Hussein Onn Malaysia (UTHM) under Research Enhancement-Graduate Grant (REGG Vot U748). The authors would also like to acknowledge UTHM for the facilities and the use of excellent testing equipment.

Author Contributions

All authors contributed to the data analysis, drafting, and critical revision of the paper, and they all agree to accept responsibility for all aspects of the work.

Disclosure of Conflict of Interest

The authors have no conflicts of interest to disclose

Compliance with Ethical Standards

The work adheres to ethical standards.

References

[1] Göbel, C. (2020). Strategies to Mitigate the Degradation of Stainless-Steel Interconnects Used in Solid Oxide Fuel Cells. (*Published Thesis*, Chalmers University of Technology, Goteborg, Sweden) pp. 7-12

[2] Radhika, D. & Nesaraj, A. S. (2013). Materials and components for low temperature solid oxide fuel cells – An overview. *Int. J. Renew. Energ. Dev*. 2(2) pp. 87–95.

[3] Dwivedi, S. (2019). ScienceDirect Solid oxide fuel cell: Materials for anode, cathode and electrolyte. *Int. J. Hydrog. Energy*. 44(45) pp. 23988-24013.

[4] Li, G., Gou, Y., Qiao, J., Sun, W., Wang, Z., & Sun, K. (2020). Recent progress of tubular solid oxide fuel cell: From materials to applications. *J. Power Sour*. 477(7) pp. 228693.

[5] Shabri, H. A., Othman, M. H. D., Mohamed, M. A., Kurniawan, T. A. & Jamil, S. M. (2021). Recent progress in metal-ceramic anode of solid oxide fuel cell for direct hydrocarbon fuel utilization: A review. *Fuel Process. Technol*. 212(5) pp. 106626.

[6]*:* Tan, K. H., Rahman, H. A. & Taib, H. (2019). Coating layer and influence of transition metal for ferritic stainless steel interconnector solid oxide fuel cell: A review. *Int. J. Hydrog. Energy*. 44(58) pp. 30591–30605.

[7] Chen, C., Zhou, H., Wang, C., L., Zhang, Y. & Zhang, K. (2021). Laser welding of ultra-high strength steel with different oscillating modes. *J. Manuf. Process*. 68 pp. 761–769.

[8] Shamsolhodaei, A., Oliveira, J. P., Schell, N., Maawad, E., Panton, B. & Zhou, Y. N. (2020). Controlling intermetallic compounds formation during laser welding of NiTi to 316L stainless steel. *Intermetallics*, 116 pp. 106656.

[9] Chevalier, S., Combemale, L., Popa, I., Chandraambhorn, S., Chandraambhorn, W., Promdirek. P., and Wongpromrat, P. (2020). Development of Solid Oxide Fuel Cell interconnect stainless steels. *Solid State Phenom*. 300 pp. 135–156.

[10] Kovacs (2018). Laser welding process specification base on welding theories. *Procedia Manuf*. 22 pp. 147–153.

[11] You, D. Y., Gao, X. D. & Katayama, S. (2014). Review of laser welding monitoring. *Sci. Technol. Weld. Join*. 19(3) pp. 181–201.

[12] Hummel, M., Schöler, C. & Gillner, A. (2021). *Metallographic Comparison for Laser Welding of Cu-ETP and CuSn6 with Laser Beam Sources of 515 nm and 1030 nm Wavelength*. (Springer Science and Business Media LLC, Springer International Publishing) pp. 1-8

[13] Hummel, M., Schöler, C., Häusler, A., Gillner, A. & Poprawe, R. (2020). New approaches on laser micro-welding of copper by using a laser beam source with a wavelength of 450 nm. *J. Adv. Join. Process*. 1(2) pp. 100012.

[14] Penilla, E. H., Deviacruz L. F., Wieg, A. T., Torres, P. M., Espitia, N. C., Sellappan, P., Kodera, Y., Aguilar, G. & Garay, J. E. (2019). Ultrafast laser welding of ceramics. *Science*. 365(6455) pp. 803–808.

[15] Auwal, S. T., Ramesh, S., Yusof, F. & Manladan, S. M. (2018). A review on laser beam welding of titanium alloys. *Int. J. Adv. Manuf. Technol.* 97(1–4) pp. 1071–1098.

[16] Zhang, B., Hong, K. M. & Shin, Y. C. (2020). Deep-learning-based porosity monitoring of laser welding process. *Manuf. Lett.* 23 pp. 62–66.

[17] Hong, K. M. & Shin, Y. C. (2017). Prospects of laser welding technology in the automotive industry: A review. *J. Mater. Process. Technol*. 245 pp. 46–69.

[18] Li, C., Huang, J., Wang, K., Chen, Z. & Liu, Q. (2019). Optimization of processing parameters of laser skin welding in vitro combining the response surface methodology with NSGAII. *Infrared Phys. Technol*. 103 pp. 103067.

[19] Kumar, G. S., Saravanan, S., Vetriselvan, R., & Raghukandan, K. (2018). Numerical and experimental studies on the effect of varied pulse energy in Nd: YAG laser welding of Monel 400 sheets. *Infrared Phys. Technol*. 93 pp. 184–191.

[20] Maio, L., Liberini, M., Campanella, D., Astarita, A., Esposito, S., Boccardi, S. & Meola, C. (2017). Infrared thermography for monitoring heat generation in a linear friction welding process of Ti6Al4V alloy. *Infrared Phys. Technology*. 81 pp. 325–338.

[21] Chateau, A., Asséko, A., Cosson, B., Schmidt, F., Le, Y., & Gilblas, R. (2015). (2017). Laser transmission welding of composites – Part B: Experimental validation of numerical model, *Infrared Phys. Technology*. 73 pp. 304–311.

[22] Yang, Y., Gao, Z. & Cao, L. (2018). Identifying optimal process parameters in deep penetration laser welding by adopting Hierarchical-Kriging model. *Infrared Phys. Technology*. 92 pp. 443–453.

[23] Shanthos K. G., Saravanan, S., Vetriselvan, R. & Raghukandan, K. (2018). Numerical and experimental studies on the effect of varied pulse energy in Nd:YAG laser welding of Monel 400 sheets. *Infrared Phys. Technol.* 93 pp. 184–191.

[24] Kumar, G. S., Raghukandan, K., Saravanan, S., & Sivagurumanikandan, N. (2019). Optimization of parameters to attain higher tensile strength in pulsed Nd: YAG laser welded Hastelloy C-276–Monel 400 sheets. *Infrared Phys. Technol*. 100 pp. 1–10.

[25] Helm, J., Schulz, A., Olowinsky, A., Dohrn, A. & Poprawe, R. (2020). Laser welding of laser-structured copper connectors for battery applications and power electronics, Weld. *World*, 64(4) pp. 611–622.

[26] Zhang, C., Li, X. & Gao, M. (2020). Effects of circular oscillating beam on heat transfer and melt flow of laser melting pool. *J. Mater. Res. Technol*. 9(4) pp. 9271–9282.

[27] Li, J., Sun, Q., Liu, Y., Zhen, Z., Sun, Q. & Feng, J. (2020). Melt flow and microstructural characteristics in beam oscillation superimposed laser welding of 304 stainless steel. *J. Manuf. Process*. 50(2) pp. 629–637.

[28] Stavridis, J., Papacharalampopoulos, A. & Stavropoulos, P. (2018). Quality assessment in laser welding: a critical review. *Int. J. Adv. Manuf. Technol.* 94(5–8) pp. 1825–1847.

[29] Noori, S. M. A., Mi, Y., Sikström, F., Ancona, A. & Choquet, I. (2021). Effect of shaped laser beam profiles on melt flow dynamics in conduction mode welding. *Int. J. Therm. Sci*. 166 pp. 1-15.

[30] Wang, Z., Oliveira, J. P., Zeng, Z., Bu, X., Peng, B. & Shao, X. (2019). Laser beam oscillating welding of 5A06 aluminum alloys: Microstructure, porosity, and mechanical properties. *Opt. Laser Technol.* 111(9) pp. 58–65.

[31] Li, S., Mi, G. & Wang, C. (2020). A study on laser beam oscillating welding characteristics for the 5083 aluminium alloy: Morphology, microstructure and mechanical properties. *J. Manuf. Process*. 53(1) pp. 12–20.

[32] Errico, V., Campanelli, S. L., Angelastro, A., Mazzarisi, M. & Casalino, G. (2020). On the feasibility of AISI 304 stainless steel laser welding with metal powder. *J. Manuf. Process*. 56(4) pp. 96–105.

[33] Liu, J., Zhu, H., Li, Z., Cui, W. & Shi, Y. (2019). Properties of the aluminum alloy joint by ultrasonic assisted laser-MIG hybrid welding. *Opt. Laser Technol*. 119(7089) pp. 105619.

[34] Zhou, X., Zhao, H., Liu, F., Yang, B., Xu, B., Chen, B. & Tan, C. (2021). Effects of beam oscillation modes on microstructure and mechanical properties of laser welded 2060 Al-Li alloy joints. *Opt. Laser Technol*. 144(7) pp. 107389.

[35] Liu, F., Tan, C., Gong, X., Wu, L., Chen, B. & Song, X. (2020). A comparative study on microstructure and mechanical properties of HG785D steel joint produced by hybrid laser-MAG welding and laser welding. *Opt. Laser Technol*. 128(8) pp. 106247.

[36] Cai, Y., Tang, F., Luo, Y., Zhang, F., Peng, Y. & Yang, S. (2020). Recognition of laser defocusing distance based on the plasma charge voltage signal. *Meas, Journal Pre-Proof.* 171 pp. 108861

[37] Atabaki, M., Ma, J., Liu, W., & Kovacevic, R. (2015). Pore formation and its mitigation during hybrid laser/arc welding of advanced high strength steel. *Mater. Des.* 67 pp. 509–521.

[38] Chandan, K., Das, M., Paul, C. P., & Singh, B. (2019). Experimental Study of Fiber Laser Weldments of 5 mm Thick Ti–6Al–4V Alloy. *Springer Singapore*. pp. 45-67

[39] Almangour, B., Grzesiak, D., Borkar, T. & Yang, J. (2017). Densification behavior, microstructural evolution, and mechanical properties of TiC/316L nanocomposites fabricated by selective laser melting. *Mater. Des.* S0264-1275 (17) pp. 30966.

[40] Mukherjee, M. (2019). Effect of build geometry and orientation on microstructure and properties of additively manufactured 316L stainless steel by laser metal deposition. *Mater.* S2589-1529 (19) pp. 30155.

[41] Peng, Y., Barzinjy, A. A., Al-rashed, A. A. A. A., Panjehpour, A., Mehrjou, M. & Afrand, M. (2019). Investigation the effect of pulsed laser parameters on the temperature distribution and joint interface properties in dissimilar laser joining of austenitic stainless steel 304 and Acrylonitrile Butadiene Styrene. *J. Manuf. Process*. 48(9) pp. 199–209.

[42] Caiazzo, F., Curcio, F., Daurelio, G. & Minutolo, F. M. C. (2004). Ti6Al4V sheets lap and butt joints carried out by CO2 laser: Mechanical and morphological characterization, *J. Mater. Process. Technol*. 149(1–3) pp. 546–552.

[43] Heydari, H. & Akbari, M. (2020). Investigating the effect of process parameters on the temperature field and mechanical properties in pulsed laser welding of Ti6Al4V alloy sheet using response surface methodology. *Infrared Phys. Technol*. 106(2) pp. 103267.

[44] Nguyen, Q., Azadkhou, A., Akbari, M., Panjehpour, A. & Karimipour, A. (2020). Experimental investigation of temperature field and fusion zone microstructure in dissimilar pulsed laser welding of austenitic stainless steel and copper. *J. Manuf. Process*. 56(2) pp. 206–215.

[45] Mosavi, A., Soleimani, A., Karimi, A., Akbari, M., Karimipour, A. & Karimipour, A. (2020). Investigating the effect of process parameters on the mechanical properties and temperature distribution in fiber laser welding of AISI304 and AISI 420 sheet using response surface methodology. *Infrared Phys. Technol*. 111(6) pp. 103478.

[46] Wan, Z., Wang, H. P., Li, J., Solomon, J., Zhu, Y. & Carlson, B. (2021). Novel measures for spatter prediction in laser welding of thin-gage zinc-coated steel. *Int. J. Heat Mass Transf.* 167 pp. 120830.

[47] Huang, S. C. & Le, M. T. (2016). Optimal design of process parameters, experimental fabrication and characterisation of a novel hybrid polymer nanocomposite. *Int. J. Mater. Prod. Technol*. 52(3/4) pp. 362.

[48] Cevik, B. & Gulenc, B. (2018). The effect of welding speed on mechanical and microstructural properties of 5754 Al (AlMg3) alloy joined by laser welding. *Mater. Res. Express*. 5(8) pp. 086520.

[49] Qianqian, G., Jiangqi, L., Ping, Y., Shunchao, J., Wenhao, H. & Jianxi, Z. (2019). Effect of steel to aluminum laser welding parameters on mechanical properties of weld beads. *Opt. Laser Technol*. 111 pp. 387–394.

[50] Khodabakhshi, F., Shah, L. H. & Gerlich, A. P. (2019). Dissimilar laser welding of an AA6022-AZ31 lap-joint by using Ni-interlayer: Novel beam-wobbling technique, processing parameters, and metallurgical characterization. *Opt. Laser Technol*. 112(9) pp. 349–362.

[51] Prabakaran, M. P. & Kannan, G. R. (2019). Optimization of laser welding process parameters in dissimilar joint of stainless steel AISI316/AISI1018 low carbon steel to attain the maximum level of mechanical properties through PWHT. *Opt. Laser Technol*. 112(11) pp. 314–322.

[52] Thawari, N., Gullipalli, C., Kumar, J. & Gupta, T. V. K. (2021). Materials Science & Engineering B Influence of buffer layer on surface and tribomechanical properties of laser cladded Stellite 6. *Mater. Sci. Eng.* 263(10) pp. 114799.

[53] Nawaz, G., Shahid, M., Singh, N. K. & Kumar, H. (2020). Experimental investigation on Ytterbium fiber laser butt welding of Inconel 625 and Duplex stainless steel 2205 thin sheets. *Opt. Laser Technol*. 126(9) pp. 106117.

[54] Lopes, J. G., & Joao, P.O. (2020). A Short Review on Welding and Joining of High Entropy Alloys. *Metals.* 10(2) 212.

[55] Akkurt, A., Şık, A. & Ovalı, İ. (2012). The Effects of Welding Parameters on the Mechanical Properties on Laser Welding of AA2024. *Pamukkale University. J. Eng. Sci*. 18 pp. 37–45.

[56] Amaya, J. M. S., Delgado, T., Gonzales- Rovira, L. & Botana, F. J. (2009). Laser welding of aluminium alloys 5083 and 6082 under conduction regime. *Appl. Surf. Sci.* 255 pp. 9512–21.

[57] Pakdil, M., Am, G. C., Kocak, M. & Erim, S. (2011). Microstructural and mechanical characterization of laser beam welded AA6056 Al-alloy. *Mater. Sci. Eng.* 528 pp. 7350–7356.

[58] Razmpoosh, M. H., Macwan, A., Biro, E. & Zhou, Y. (2018). Surface & Coatings Technology Effect of coating weight on fiber laser welding of Galvanneal-coated 22MnB5 press hardening steel. *Surf. Coat. Technol.* 337 pp. 536–543.

[59] Kolubaev, A. V, Sizova, O. V, Fortuna, S. V, Vorontsov, A. V, Ivanov, A. N. & Kolubaev, E. A. (2020). Weld structure of low-carbon structural steel formed by ultrasonic-assisted laser welding. *J. Constr. Steel Res.*172 pp. 106-190.

[60] Köse, C. & Topal, C. (2019). Laser welding of AISI 410S ferritic stainless steel Laser welding of AISI 410S ferritic stainless steel. *Mater. Res. Express.* 6 pp. 08654.